RFCM FOR DATA ASSOCIATION AND MULTITARGET TRACKING USING 3D RADAR

Chun-Nien Chan and Carrson C. Fung

Dept. of Electronics Engineering, National Chiao Tung University, Hsinchu, 300 Taiwan

ABSTRACT

Performance of object classification using 3D automotive radar relies on accurate data association and multitarget tracking, which are greatly affected by data bias and proximity of objects to each other. A regularized fuzzy c-means (RFCM) algorithm is proposed herein to resolve the data association uncertainty problem that has shown to outperform the conventional FCM algorithm. The proposed method exploits results from the companion tracker to increase performance robustness. Simulation results using simulated and field data have proven the efficacy of the proposed method.

***Index Terms*—** Autonomous driving, ADAS, data association, multitarget tracking, regularized fuzzy c-means

1. INTRODUCTION

Autonomous driving technology has long been pursued by robotics and machine learning researchers. Despite the current thrust toward using video and LiDAR signals to perform tracking, mapping, and classification, automotive radar remains a crucial part of an overall automotive system due to its extensive range and ability to accurately detect objects in unfavorable weather conditions. Unfortunately, its low resolution precludes its use beyond basic detection. Recently, a 3D 79 GHz radar is capable of capturing detail information about vehicular objects which can provide detail features about the object-of-interest such as cycle number, received signal power, range, azimuth and elevation angle, and radial velocity. Initial simulations have shown promising results in terms of using it for object classification. However, solving the data association uncertainty and subsequent multitarget tracking problems [1, 2] are crucial before such a system can be deployed for object classification. The main challenge is to estimate the state of unknown and time-varying number of targets from a set of noisy and uncertain observations.

Data association uncertainty arises when remote sensors such as radar output measurements whose origin is uncertain and not necessarily originated from the object-of-interest. Using such measurements in tracking will lead to track loss. Several strategies have been proposed in literature to tackle this problem, such as Nearest Neighbor (NN) [3], Joint Probabilistic Data Association (JPDA) [4–6], and deep learning methods [7]. NN technique is computational efficient but not suitable for intensive multitarget scenario. The JPDA is considered ideal in a cluttered environment but the increase in computational complexity when the number of detected targets increases is not affordable for practical usage in low-cost embedded systems such as ADAS. Deep learning based methods have been actively pursued recently in the field of multitarget tracking (MTT) due to its superior performance over traditional techniques such as extended Kalman filtering (EKF). However, the lack of a systematic way to choose a proper deep learning model and the need to estimate large number of parameters, which requires vast amount of training data and time, pose a serious obstacle for designers. Recently, improved fuzzy cluster means (FCM) algorithm based methods [8–10] have been proposed for MTT in wireless sensor network. Its computational efficiency makes it an attractive alternative to optimized methods such as JPDA.

A regularized FCM (RFCM) method is proposed herein for solving the data association uncertainty problem for the 3D 79 GHz radar. The proposed method attempts to alleviate this problem by taking the interaction between targets into account and correct the estimation of state in the tracking algorithm in a sequential manner. This results in a model data-driven based joint data association and MTT algorithm which enables objects that are close in proximity in one or several cycles to be segmented and tracked, which the FCM fails to do.

Notations: Upper (lower) bold face letters indicate matrices (column vectors). Superscript ^{H} denotes Hermitian, ^{T} denotes transposition. $Diag(\mathbf{a})$ creates an $N \times N$ diagonal matrix using the elements of $\mathbf{a} \in \mathbb{C}^N$. $\|\cdot\|_2$ denotes ℓ_2 norm.

2. FCM ALGORITHM AND MTT

2.1. Conventional FCM

The FCM [11] is one of the most popular algorithms for cluster analysis. FCM focuses on obtaining a fuzzy c-partition for the given data set by minimizing an objective function. The FCM algorithm is particularly suitable for segmenting noisy data because of the incorporation of probability measure called membership function which makes the clustering

The work described in this paper has been supported by the Ministry of Science and Technology Grant 106-2221-E-009-087 and Winstron NeWeb Corporation.

more robust.

The FCM algorithm attempts to find C cluster centroids that can optimally represent N data points $\mathbf{x}_i$ (in the context of the 3D radar, $\mathbf{x}_i$ can consists of features $[x_i \;\; y_i \;\; v_{x_i} \;\; v_{y,i}]^T$ described in Sec. 2.2), for $i = 1, \ldots, N$ by iteratively solving

$$\min_{\mathbf{c}_i} \sum_{j=1}^{N} \sum_{i=1}^{C} u_{i,j}^m d_{i,j}^2, \tag{1}$$

with $d_{i,j}^2 \triangleq \|\mathbf{x}_j - \mathbf{c}_i\|_2^2$ and $\mathbf{c}_i$ as the centroid. $u_{i,j} = \frac{1}{\sum_{k=1}^{C}(\frac{d_{i,j}}{d_{k,j}})^{\frac{2}{m-1}}}$ denotes the membership function that is fixed when solving (1) and is obtained in an iterative manner after (1) has been solved. It is clear that $u_{i,j}$ is an inverse probability measuring the likelihood of the jth data point being associated with the ith centroid obtained in the previous iteration. This allows clustering results from previous iteration to influence current results to lessen the effect of data bias in the current iteration. $m > 1$ is a weighting factor controlling the cluster fuzziness. Since (1) is a convex problem, the solution can easily be obtained in closed form as $\widehat{\mathbf{c}}_i = \frac{\sum_{j=1}^{n} u_{i,j}^m \mathbf{x}_j}{\sum_{j=1}^{n} u_{i,j}^m}$.

2.2. Tracking with FCM

In MTT, since the number of objects is unknown, the proposed method uses the density-based spatial clustering of applications with noise, or DBSCAN [12], algorithm to obtain initial C clusters at initial cycle t using the location and velocity feature, with respect to the horizontal axis x and y. Assume there are N points in the current cycle t, the jth feature vector for the jth data point becomes $\left[x_j \;\; y_j \;\; v_{x_j} \;\; v_{y,j}\right]^T$, for $j = 1, 2, \ldots, N$, where x_j and y_j denote the x and y coordinate of the jth data point, and $v_{x,j}$ and v_{y_j} denote the x and y components of the radial velocity, respectively, of the jth data point. Assuming the DBSCAN algorithm outputs C number of centroids, denoted as $\widehat{\mathbf{c}}_i(t) \triangleq [x_i \;\; y_i \;\; v_{x_i} \;\; v_{y,i}]^T$, for $i = 1, 2, \ldots, C$, it is then used as input state vector and observation (x_i, y_i only) for the EKF to obtain path information about each of the ith centroids (objects). The results of the EKF, denoted as $\mathbf{c}_i^p(t) \triangleq \left[x_i^p \;\; y_i^p \;\; v_{x_i}^p \;\; v_{y,i}^p\right]^T$, shall then be used as initial centroids for the RFCM algorithm (Sec. 3) to determine the new centroids $\widehat{\mathbf{c}}_i(t+1)$ in the next cycle $t+1$.

When objects are relatively close to each other, it is conceivable that their point clouds will overlap, making it difficult for the FCM algorithm to generate accurate membership. The RFCM described in the next section is proposed to further enhance segmentation performance.

3. REGULARIZED FCM

Figs. 1 shows that when objects are close to each other, the point clouds of different objects will overlap. Incorporating the proposed RFCM into the association algorithm can greatly mitigate this problem since the RFCM, as compared to the conventional FCM, contains two additional regularization terms in its design formulation which exploit the result from the tracking algorithm so that the proposed RFCM algorithm can properly trade off between trusting the (noisy) data and result predicted by the EKF in determining the centroid. Precisely speaking, the RFCM attempts to find the optimal ith centroid, $\widehat{\mathbf{c}}_i$, for the jth point $\mathbf{x}_j$ by solving

$$\min_{\mathbf{c}_i} \sum_{j=1}^{N} \left(\sum_{i=1}^{C} u_{i,j}^m d_{i,j}^2 - \frac{f_1}{C-1} \sum_{\substack{k=1 \\ k \neq i}}^{C} \frac{\|\mathbf{c}_i - \mathbf{c}_k^p\|_2^2}{\|\mathbf{c}_i^p - \mathbf{c}_k^p\|_2^2} + f_2(d_i)\|\mathbf{c}_i - \mathbf{c}_i^p\|_2^2 \right), \tag{2}$$

where $\mathbf{c}_i^p$ and $\mathbf{c}_k^p$ are the cluster center for the ith and kth object, respectively, obtained from the EKF; f_1 and $f_2(d_i)$ are regularization parameters; the latter of which is a function of the distance d_i between the radar and the ith predicted centroid $\mathbf{c}_i^p$. The inclusion of the second term in (2) allows the RFCM algorithm to design $\widehat{\mathbf{c}}_i$ such that it is not close to $\mathbf{c}_k^p$. Similarly, the third term in (2) allows $\widehat{\mathbf{c}}_i$ to be attracted to $\mathbf{c}_i^p$, that is, favoring the result from the EKF. In other words, these two terms allow the EKF to impose some influence on the determination of $\widehat{\mathbf{c}}_i$ so that in case $\mathbf{x}_j$ for $j = 1, \ldots, N$ are noisy or close to each other so that point clouds belonging to different objects overlap, the RFCM can offer additional robustness so that points are not incorrectly assigned.

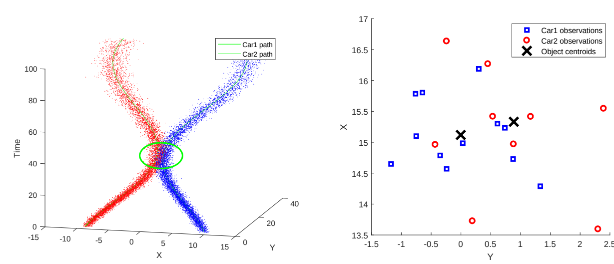

(a) Points of 2 objects. (b) Point clouds overlap.

Fig. 1. Point clouds overlap when two objects are close to each other. Area circled in green in Fig. 1(a) is enlarged in Fig. 1(b).

Unfortunately (2) is non-convex, but it can be reformulated into a convex problem as

$$\min_{\mathbf{c}_i} \sum_{j=1}^{N} \left(\sum_{i=1}^{C} u_{i,j}^m d_{i,j}^2 + \frac{f_1}{C-1} \sum_{\substack{k=1 \\ k \neq i}}^{C} \frac{\|\mathbf{c}_i - \mathbf{c}_{i,k}^p\|_2^2}{\|\mathbf{c}_i^p - \mathbf{c}_k^p\|_2^2} + f_2(d_i)\|\mathbf{c}_i - \mathbf{c}_i^p\|_2^2 \right), \tag{3}$$

where $\mathbf{c}_{i,k}^p = (\mathbf{c}_i^p - \mathbf{c}_k^p) + \mathbf{c}_i^p$ defines the mirror point of $\mathbf{c}_k^p$ with respect to $\mathbf{c}_i^p$ as illustrated in Fig. 2 assuming the centroids are two dimensional. Hence, the new formulation of the RFCM encourages $\mathbf{c}_i$ to be closer to the mirror point $\mathbf{c}_{i,k}^p$.

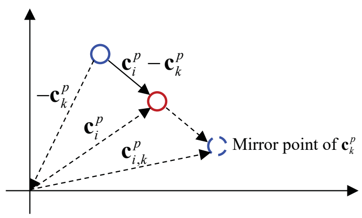

Fig. 2. Mirror point $\mathbf{c}_{i,k}^p$ of $\mathbf{c}_k^p$ with respect to $\mathbf{c}_i^p$ (the mirror).

The normalization factor $\|\mathbf{c}_i^p - \mathbf{c}_k^p\|_2^2$ in (3) is needed because when there are multiple objects that need to be clustered, as illustrated in Fig. 3 where $C = 3$, if the normalization factor is not included, then $\mathbf{c}_i$ will be drawn closer to the mirror point $\mathbf{c}_{i,\ell}^p$ as $\|\mathbf{c}_i - \mathbf{c}_{i,\ell}^p\|_2 > \|\mathbf{c}_i - \mathbf{c}_{i,k}^p\|_2$. However, this will bring $\mathbf{c}_i$ closer to $\mathbf{c}_k^p$, which is undesirable. If the normalization factor is included, since $\|\mathbf{c}_i^p - \mathbf{c}_{i,k}^p\|_2 < \|\mathbf{c}_i^p - \mathbf{c}_{i,\ell}^p\|_2$, then $\mathbf{c}_i$ will now be drawn closer to $\mathbf{c}_{i,k}^p$. Even though $\mathbf{c}_i$ will be closer to $\mathbf{c}_\ell^p$, since $\mathbf{c}_\ell^p$ is further away, there will be no collision between the cluster as in the previous case.

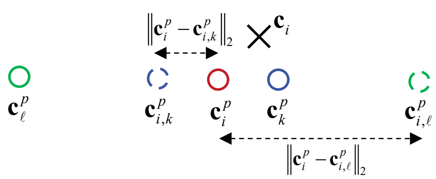

Fig. 3. Influence of $\|\mathbf{c}_i^p - \mathbf{c}_{i,k}^p\|_2$ and $\|\mathbf{c}_i^p - \mathbf{c}_{i,\ell}^p\|_2$.

Since the accuracy of the EKF hinges on N, as d_i increases, N will decrease, thus adversely affecting the accuracy of the EKF. Hence, f_1 and $f_2(d_i)$ should be a function of d_i. Since the importance of the regularization terms in (3) are relative to each other, initial simulations have shown that good results can be obtained when only one of the parameters is a function of d_i. Therefore, f_1 is chosen to be a constant that needs to be manually tuned and $f_2(d_i) = \alpha \cdot d$, with α being a parameter that also requires fine tuning.

$\widehat{\mathbf{c}}_i$ can be found analytically by differentiating (3) and setting the result to zero, so that

$$\widehat{\mathbf{c}}_i = \frac{\sum_{j=1}^N u_{i,j}^m \mathbf{x}_j + \frac{f_1}{C-1}\sum_{\substack{k=1\\k\neq j}}^C \frac{\mathbf{c}_{i,k}^p}{\|\mathbf{c}_i^p - \mathbf{c}_k^p\|_2^2} + f_2(d_i)\mathbf{c}_i^p}{\sum_{j=1}^N u_{i,j}^m + \frac{f_1}{C-1}\sum_{\substack{k=1\\k\neq j}}^C \frac{1}{\|\mathbf{c}_i^p - \mathbf{c}_k^p\|_2^2} + f_2(d_i)}. \tag{4}$$

4. SIMULATION RESULTS

Due to the lack of ground truth data, simulations were carried out using both simulated and field data from the 3D radar. All tracking results are generated using the EKF [13, pp. 449]. The process noise covariance matrix $\mathbf{Q} = Diag([0, 0, 0.0001, 0.0001])$ and the observation noise covariance matrix $\mathbf{C} = Diag([0.01, 0.005])$, and $m = 3$ for the (R)FCM.

Fig. 4 shows the clustering and tracking result for simulated data using the conventional FCM and the proposed RFCM methods. The simulation attempts to cluster and track two objects (two cars) initially located at $y = 0$ moving away from the radar. In the simulation, the paths of the two vehicles follow the shape of a cosine function, and will be closest to each other at cycle number (time) 415. Comparing Figs. 4(b) with 4(c), which show only one instance of the experiment, the RFCM is able to sustain proper tracking of the objects while the FCM provided incorrect tracks after cycle 415. The result is quantified by measuring the mean-squared error (MSE) vs. the cycle number. The MSE at cycle t is computed as $\mathrm{MSE}(t) = \frac{1}{M}\sum_{m=1}^M \sum_{i=1}^C \|\mathbf{b}_i(t) - \widehat{\mathbf{b}}_i(t)\|_2^2$, where $\mathbf{b}_i(t)$ and $\widehat{\mathbf{b}}_i(t)$ contain the first two elements of $\mathbf{c}_i(t)$ and $\widehat{\mathbf{c}}_i(t)$, respectively, with $\mathbf{c}_i(t)$ denoting the actual centroid at the tth cycle. $M = 500$ denotes the number of Monte Carlo trials. As the MSE results in Fig. 5 have shown, the RFCM performs almost identically with the FCM at the first 400 to 500 cycles, i.e. when the objects are relatively close to the radar. After that, the RFCM starts to dramatically outperform the FCM because the latter is more sensitive to error due to increases in the point cloud radius. The increase in MSE as d_i increases can be attributed to the fact that the predicted paths of the two objects can cross (similar to the behavior observed in Fig. 4(b)), with less occurrences for the RFCM.

Fig. 6 shows the results of using the association algorithm with conventional FCM and the proposed RFCM method to segment and track two objects-of-interest, a pedestrian and a car moving side by side, using actual field data collected using the 3D radar. As depicted in the figure, there are numerous tracks because of reflected signal from other non-object-of-interest. The FCM and RFCM were initialized by computing the ideal centroid, similar to the results shown in Fig. 4. A third graph is added using the DBSCAN and RFCM algorithm. ε and minimum number of neighbors are parameters used in the DBSCAN algorithm. Comparing Fig. 6(a) with 6(b), the RFCM is better able to track objects stably. Unfortunately, using the DBSCAN algorithm to initialize the clusters, it is only possible to track one object because the RFCM treats both the pedestrian and car as one object. This is because the point cloud of the two objects dramatically overlap at the beginning few cycles so that there is no way to distinguish two objects as d_i increases, even if the point cloud of the two objects become further apart. This can be amended by initiating DBSCAN at every cycle so that new cluster can be identified at every cycle.

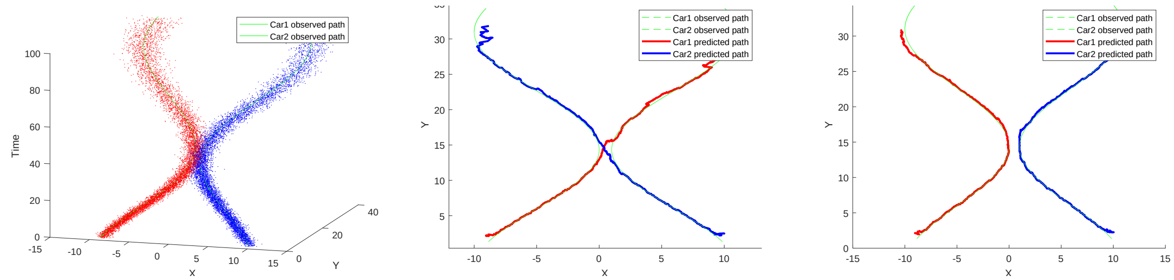

(a) Simulated point clouds of two different objects.

(b) FCM for data shown in Fig. 4(a).

(c) RFCM for data shown in Fig. 4(a). $f_1 = 0.6$ and $\alpha = 0.003$.

Fig. 4. Clustering and tracking result of simulated curve data. Green line in all figures indicate actual paths of the objects (2 cars). Red line in Figs. 4(b) and 4(c) indicates the predicted path for the objects on the left, and blue line for the object on the right. The radar is located at $x = y = 0$. The two objects move from $y = 0$ upward away from the radar, and travel a cosine-like path.

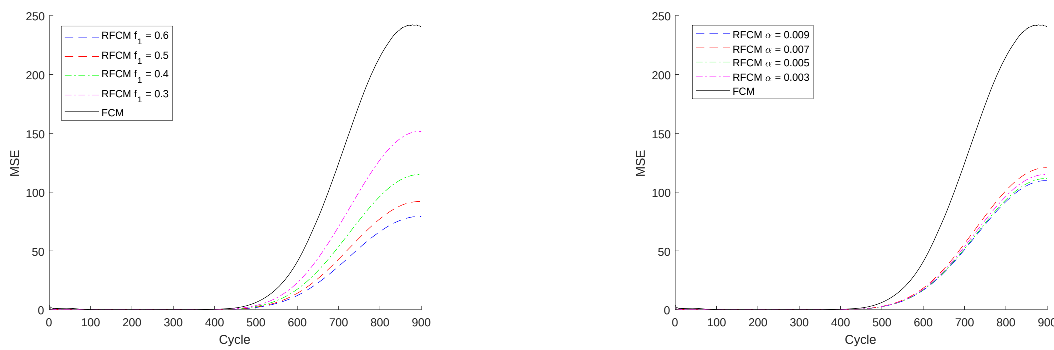

(a) MSE vs. cycle time for FCM and RFCM with $\alpha = 0.003$ Four values of $f_1 = 0.3$, 0.4, 0.5, and 0.6 are used for the RFCM.

(b) MSE vs. cycle time for FCM and RFCM with $f_1 = 0.4$. Four different values of $\alpha = 0.003$, 0.005, 0.007, and 0.009 are used for the RFCM.

Fig. 5. MSE vs. cycle time results of clustering and tracking result for simulated curve data shown in Fig. 4 using different parameter values for the RFCM.

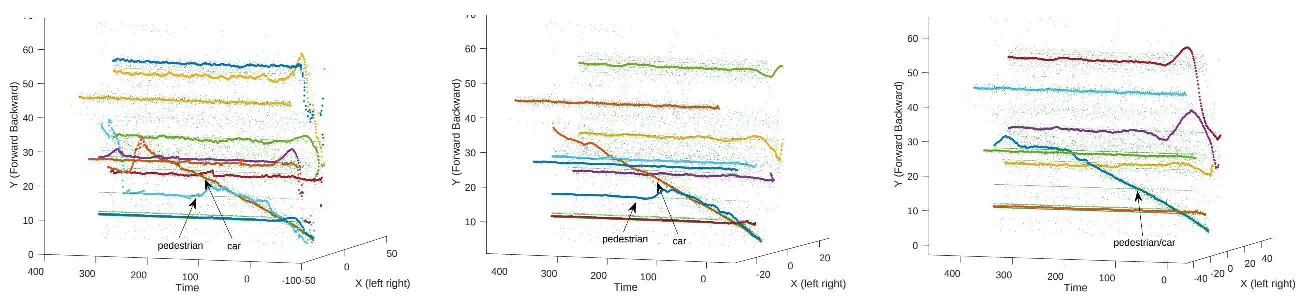

(a) FCM.

(b) RFCM.

(c) DBSCAN initialization with RFCM.

Fig. 6. Clustering and tracking result for actual field data. Objects-of-interest consist of a car and pedestrian moving side by side. $f_1 = 0.25$ and $\alpha = 0.009$ for the RFCM. $\varepsilon = 1.5$ and minimum number of points = 3 for the DBSCAN.

5. CONCLUSION

A RFCM algorithm is proposed herein to solve the data association uncertainty problem for 3D radar, with the ultimate goal of achieving object classification for autonomous driving. The proposed RFCM method is able to outperform the conventional FCM method in improving data association performance, which leads to improved tracking performance using the EKF. Simulation results using simulated and field data have proven the efficacy of the proposed method.

6. REFERENCES

[1] B.-N. Vo *et al.*, "Multitarget tracking," *Wiley Encyclopedia of Electrical and Electronics Engineering*, Sep. 2015.

[2] C. Qiu *et al.*, "A survey of motion-based multitarget tracking methods," *Progress In Electromagnetics Research B*, vol. 62, pp. 195-223, 2015.

[3] J.I. Cox, "A review of statistical data association techniques for motion correspondence," *International Journal of Computer Vision*, vol. 10(1), pp. 53-66, 1993.

[4] T.E. Fortmann, Y. Bar-Shalom and M. Scheffe, "Multitarget tracking using joint probabilistic data association," *Proc. of the 19th IEEE Conf. on Decision and Control*, pp. 807-812, 1980.

[5] T.E. Fortmann, Y. Bar-Shalom and M. Scheffe, "Sonar tracking of multiple targets using joint probabilistic data association," *IEEE Journal of Oceanic Engineering*, vol. 8(3), pp. 173-184, 1983.

[6] S.H. Rezatofighi *et al.*, "Joint probabilistic data association revisited," *Proc. of the IEEE Intl. Conf. on Computer Vision*, Santiago, Chile, pp. 3047-3055, Dec. 2015.

[7] A. Milan *et al.* , "Online Multi-Target Tracking Using Recurrent Neural Networks," *Proc. of the 31st AAAI Conf. on Artificial Intelligence*, San Francisco, CA, USA, pp. 4225-4232, Feb. 2017.

[8] A.M. Abdel-Aziz, "An all-neighbor fuzzy association approach in multisensor-multitarget tracking systems," *Proc. of the 21st National Radio Science Conference*, Cairo, Egypt, Mar. 2004.

[9] L. Fan, H. Wang and H. Wang, "A solution of multitarget tracking based on FCM algorithm in WSN," *Proc. of the Fourth Annual IEEE Intl. Pervasive Computing and Communications Workshops,*, Pisa, Italy, Mar. 2006.

[10] M. Liu, D. Huang and H. Gao, "Multi-target tracking algorithm based on rough and precision association mixing FCM in WSN," *Proc. of the Intl. Conf. on Computational Intelligence and Natural Computing*, Wuhan, China, vol. 2, pp. 67-71, Jun. 2009.

[11] J.C. Bezdek and J.C. Dunn, "Optimal fuzzy partitions: A heuristic for estimating the parameters in a mixture of normal distributions," *IEEE Trans. on Computers*, vol. C-24(8), pp. 835-838, Aug. 1975.

[12] M. Ester *et al.*, "A density-based algorithm for discovering clusters in large spatial databases with noise," *Proc. of the 2nd Intl. Conf. on Knowledge Discovery and Data Mining*, AAAI Press, pp. 226-231, 1996.

[13] S.M. Kay, *Statistical Signal Processing: Estimation Theory*, Prentice Hall, 1993.